Journal of Additive Manufacturing Technologies
DOI: 10.18416/JAMTECH.2111563

Infinite Science | Publishing

Distortion and dimensional deviation of Inconel 718 auxetic structures produced by DMLM

O. Gülcan[1*], K. Günaydın[1]

[1] *General Electric Aviation, Kocaeli, Turkey*
[*] *Corresponding author, email: ogulcan1981@gmail.com*

Abstract

Due to their geometrical shapes, auxetic structures expand laterally when stretched and contract laterally when compressed. These structures find their usages in different industries where high energy absorption, toughness, flexural rigidity or buckling under pure bending are required. Additively manufactured parts have some amount of distortion due to the nature of the process and this distortion has a great influence on mechanical properties of the final part. Knowledge about distortion characteristics of thin-walled lattice structures manufactured by additive manufacturing is very important to better estimate and evaluate the mechanical behavior of these parts when used in industrial applications. For this purpose, this study focuses on distortion characteristics of IN718 re-entrant, anti-tetrachiral and honeycomb lattice structures manufactured by powder bed fusion additive manufacturing. To investigate distortion and geometrical deviations produced thin-walled lattice structures were scanned in two conditions with blue light device: just after printing when parts are still on build plate, and just after removing the specimens from build plate and splitting them into three pieces. Printed structure geometries were compared with the original CAD model and finite element analysis. Numerical results showed acceptable results in the directions, in which the re-coater effect is inconsiderable.

Keywords: Lattice structures, Powder bed fusion additive manufacturing, Blue light scan, Geometric deviation, distortion.

1. Introduction

When a part is subjected to tensile loading, it extends in longitudinal direction and contracts in lateral direction. The ratio of contraction strain to extension strain is called Poisson's ratio. Poisson's ratio of most materials is close to 1/3 but in rubbery materials, it approaches to 1/2. Apart from these materials, some materials show negative Poisson's ratio characteristics (1).

Lakes was first invented negative Poisson's ratio foams in 1987 [2]. In most of the published papers, negative Poisson's ratio materials have also been called auxetic materials / structures (2,3). Thanks to improvements in the additive manufacturing technologies, lattice auxetic structures have drawn attention due to their improved energy absorption capability (4). Many different types of negative Poisson's ratio geometries were proposed. However, prevalent auxetic lattice structures are re-entrant and anti-tetrachiral structures, which have different deformation mechanisms in accordance with their unit cell geometry (5,6). Besides the energy absorption capabilities, auxetic structures show high mechanical strength and viscoelastic behaviors and due to these properties, they are used in different industries such as aviation, biomedical and automotive (7,8).

In recent years, there has been an increase in studies on the manufacturing of these structures with powder bed fusion additive manufacturing processes. Direct metal laser melting (DMLM) is the one of the prevalent powder bed fusion processes. In this process, CAD geometry is sliced into multiple layers and for each layer, powder is laid onto the machine platform and the laser is used to melt the powder.

Several studies have been conducted to elaborate geometrical deviation and distortion of additively printed thin-walled lattice structures. The dimensional deviation does not solely cause dimensional problems, but it influences the mechanical properties of the structure. Dallago et al. stated that lattice structures manufactured by additive manufacturing show dimensional differences between the produced part and the designed part and concluded that these differences decrease the elastic modulus of the produced part (9). Dimensional accuracy of additively printed structures is dependent on build parameters such as laser power, laser spot size, laser pulse duration and frequency, powder particle size and morphology, scan speed and spacing, layer thickness, scan pattern, powder bed temperature, powder feed temperature and heat dissipation during process. There are some studies, which clarifies the effect of build parameters on dimensional accuracy. Bartolomeu et al. attributed the dimensional difference in the Ti6Al4V lattice structures manufactured by DMLM to the differences in the powder particle size and the heat transfer from the melt pool to the surrounding powder (7,10). Ran et al. stated that in Ti6Al4V lattice structures, the porosities of 500, 700 and 900 μm diameters added in the design came

out as 401, 607 and 801 µm after production, and the reason for this was the adhesion of the powder to the surface due to the heat transfer between the powder and the solid part (11). Wang et al. stated that dimensional accuracy of different geometrical features were affected by laser penetration, laser beam width, stair step effect and non-fully melted powder adhesion (12). Calignano et al. stated that dimensional accuracy of AlSi10Mg parts produced by laser powder bed fusion depended on conversion from CAD file to stl file, process parameters and build direction (13). In addition, build orientation strongly dominates the geometrical deviation. Ahmed et al. investigated dimensional accuracy and distortion of thin wall AlSi10Mg features produced by selective laser melting. Experimental results revealed that horizontal and vertical dimensions showed 0.05 mm and 0.258 mm maximum dimensional errors, respectively. They stated that both dimensional errors and distortions decreased with increasing sample thickness (14). Moreover, the dimension of the intended geometry influences the geometrical deviations. Yan et al. investigated AISI 316L stainless steel gyroid lattice structures with different volume fractions (6, 8, 10 and 12 %) manufactured by DMLM and stated that strut sizes came out to be higher than the designed due to adhesion of non-fully melted powders (15). Maran et al. investigated the dimensional deviations of re-entrant structures manufactured from maraging steel (MS1) with selective laser melting. They observed that dimensional accuracy of struts thicknesses decreased with decreasing build orientation angle. On the other hand, length accuracy increased with decreasing build orientation angle (16).

Knowledge about the distortions and dimensional differences that may be observed when the auxetic materials are manufactured by DMLM will give design engineers an ability of making design changes accordingly so that maximum benefit from high energy absorption and mechanical strength of auxetic materials in industrial applications can be obtained. Furthermore, to the authors' knowledge, no other study has addressed the geometrical deviation and distortion characteristics of thin-walled lattice cells which are split into three parts instead of separately production to reduce the production costs and time. For this purpose, in the present study, re-entrant, anti-tetrachiral and honeycomb lattice structures were manufactured by DMLM and three-dimensional scanning of the parts before after removing from the build plate and after splitting into three parts was performed and the after results were compared with the intended CAD geometry. Additionally, after removal scan results were compared with numerical analysis results for a validation study.

2. Material and methods

2.1. Specimen design and preparation for manufacturing

Three different auxetic structures (re-entrant, anti-tetrachiral and honeycomb) were modeled using Siemens NX software. Images and specific dimensions of the models are shown in Fig 1.

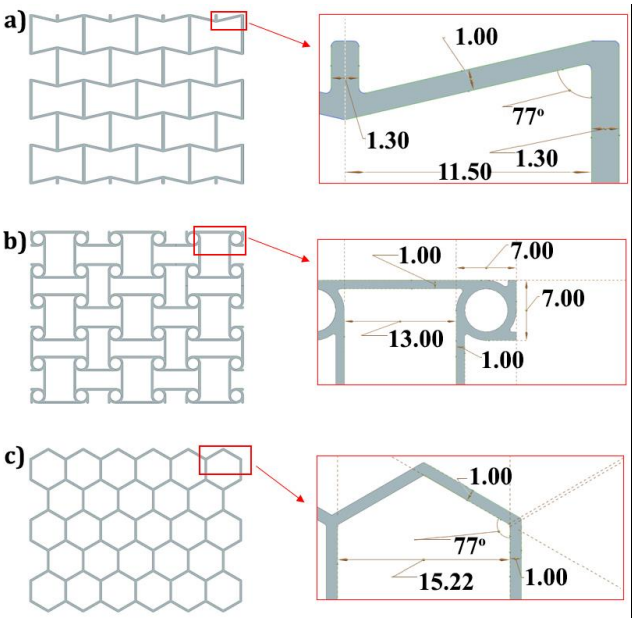

Fig 1. a) Re-entrant, b) anti-tetrachiral and c) honeycomb auxetic structures (all dimensions are in mm).

The designed specimens were placed on the build plate as in Fig 2. In order to shorten the printing time, each sample was designed with a height of 50 mm and it was planned to divide them into three parts of 15 mm by wire electrical discharge machining (WEDM) after printing. An additional 5 mm was put as a tolerance for problems that may occur during WEDM.

2.2. Specimen manufacturing

The specimens were manufactured using the Concept Laser M2 machine from Inconel 718 material. The chemical composition of the Inconel 718 material used in production is shown in Table 1, and the standard vendor process parameters were used as presented in Table 2.

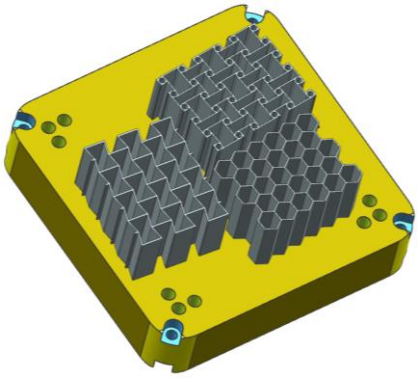

Fig 2. Build layout of specimens.

Table 1. Chemical composition of Inconel 718 wt%.

Ni	Cr	Nb	Mo	Ti	Mn	Si	Al	Fe
53.00	18.50	5.00	3.00	0.66	3.00	0.35	0.35	Bal

Table 2. Processing parameters of the AM Inconel 718 (17).

	Laser power (W)	Laser scan speed (mm/s)	Laser spot size (µm)
Skin	160	800	80
Core	160	680	53

2.1. WEDM and 3D scanning

The manufactured specimens were scanned in three stages with ATOS ScanBox 4105 blue light device. GOM Inspect software was employed to elaborate and investigate the scan results. The dimensional accuracy of the scan is ranging between 15 to 20 µm for small volume (<100x100x100 mm) structures and 30 to 40 µm for high volume ones. For aligning the scanned geometry (actual geometry) with the CAD geometry (nominal geometry) GOM Inspect pre-alignment option and datum planes were employed. GF Agiecharmill WEDM machine with 0.3 mm wire thickness and 5 mm/min average cutting speed was used for removing specimens from the build plate and then cutting them into three pieces. The relevant stages are shown in Fig 3. WEDM cutting direction for the build plate removal was assigned as the same direction with re-coater direction as shown in Fig 5.

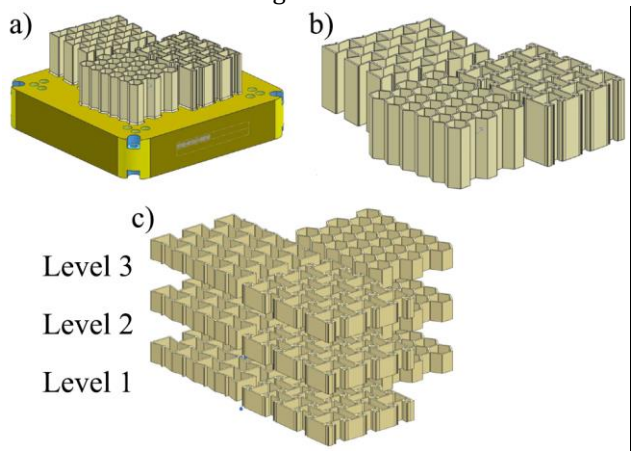

Fig 3. Three stages of the specimens: a) after printing, before removing from build plate, b) after removing build plate, before cutting into three parts, c) after cutting into three parts.

First, all the lattice structures were removed from the plate with WEDM, and then every lattice structure was split into three parts. After the thin-walled lattice structures removal process from the build plate, lattice structures were placed in their build layout positions for better scan and alignment options.

2.1. Numerical Analysis

For the thermomechanical numerical analysis, Simufact Additive 4.1 commercial code was utilized. The build plate was selected as 316L steel plate as it was in the production with a dimension of 245x245x50 mm. Build plate and lattice structures were discretized with voxel mesh elements. For the build plate, it was decided to use 3 mm mesh size and 1 mm for the lattice structures. The total number of the voxel elements and nodes were 336190 and 530129, respectively. The element sizes were defined according to the convergence and computational cost studies. The cutting option was enabled with a tolerance of 3.3 mm for simulating the geometrical deviation after structures are removed from the build plate.

3. Results and discussion

The manufactured specimens are shown in Fig 4. No clear production problem was found in visual check. A direction notation illustration is exhibited in Fig 5., and re-coater and WEDM cutting direction are shown as in the East direction. All the results were evaluated according to the notation. In addition, the angled layout of lattice structures is stemming from the reduction of drag force of re-coater and providing build layout.

In Fig 6., numerical results and scan results are compared in each direction in the limit of 1.25 mm to -1.25 mm. In the S direction, geometrical deviations for the honeycomb structure is reaching 0.75 mm. However, there was a negative deviation in the numerical analysis results. Similar results can be observed in the W direction. The reason for the positive deviation in the S direction can be explained by the drag force of the re-coater and sweeping the powder in the S direction. However, the reason why the positive deviation was occurred in the S direction is the angle of the lattice structures. The angle between re-coater direction causes the sweeping powders in the S direction. The numerical analysis cannot capture these positive deviations due to the lack of analyzing the re-coater direction. As to the N and E directions, it is changing between 0.50 and -0.25 for the numerical analysis. However, the deviation values for the scan results are varying between 0.25 and -1.00. Moreover, numerical results can display varying results throughout the lattice structures height, but this trend is not sharp in the scan results as is in the numerical results.

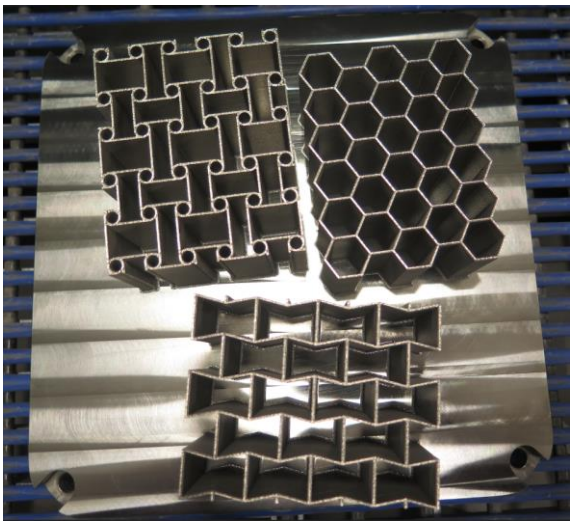

Fig 4. Produced specimens.

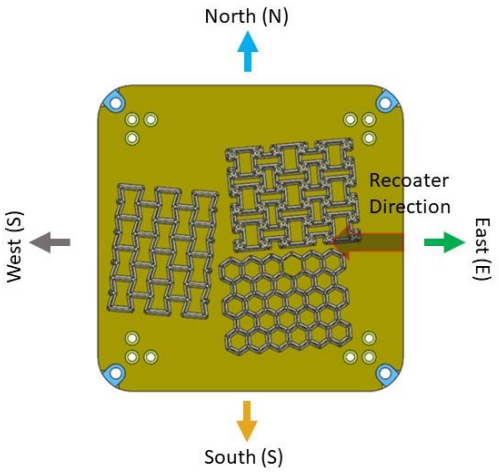

Fig 5. Directions and re-coater direction.

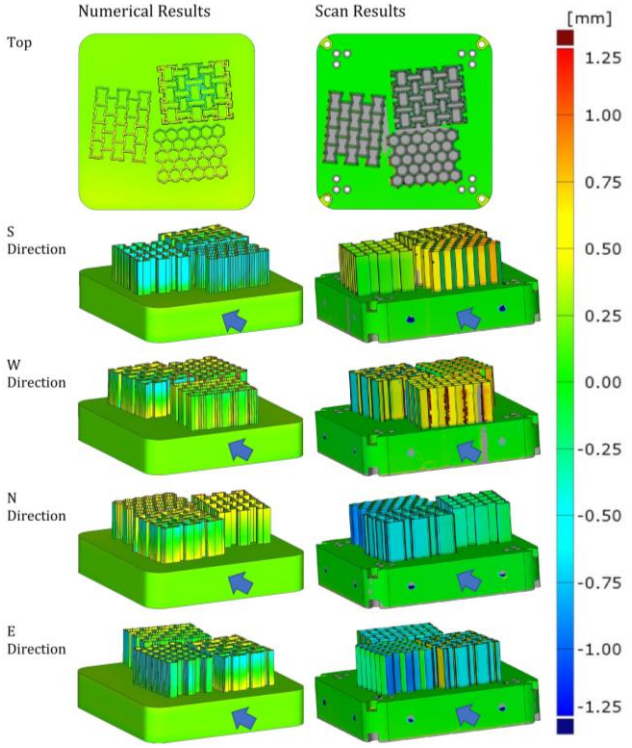

Fig 6. Scan and numerical results comparison after build plate removal.

The scan results of three pieces re-entrant lattice structures are presented in Fig 7. All pieces were scanned, and their deviations are exhibited. Level 1 addresses the first part in which it has contact with the build plate. According to scan results, distortion can be observed mostly in level 3 and then level 2. In E and W direction of level 1 and 3, the positive deviation is monitored around 0.40 mm at the bottom however, negative deviation can be observed at the top of the cells reaching to -0.4 mm. This situation indicates the tapered shape of the lattice structures. The positive deviation in the Z direction is an expected result due to the nature of additive manufacturing. Sharp edges are weak in terms of heat dissipation and cause high distortion.

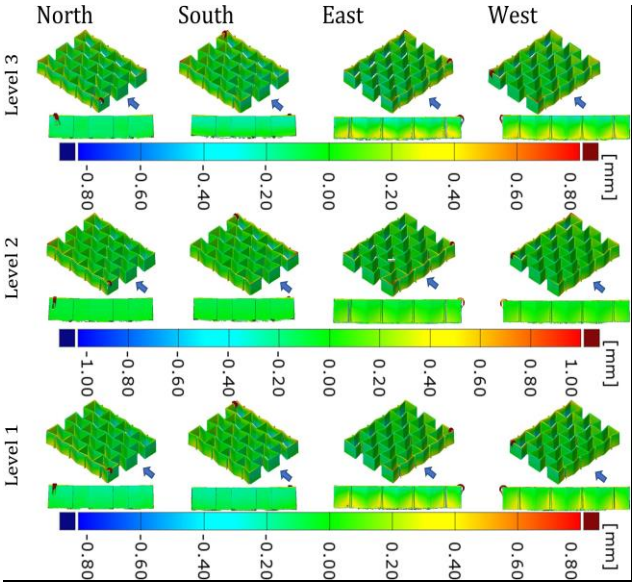

Fig 7. Scan results after splitting the re-entrant structure into three pieces.

In Fig 8., scan results of three pieces honeycomb lattice structures are shown. The positive deviation in the Z direction is not severe as is seen in the re-entrant lattice structures. Honeycomb lattice structure showed better equally distributed geometrical deviation in comparison with other lattice structures due to its unique topology. As to the taperness, it is not dominated as is in the re-entrant lattice structures, and the deviations vary in the range of 0.40 to -40 mm.

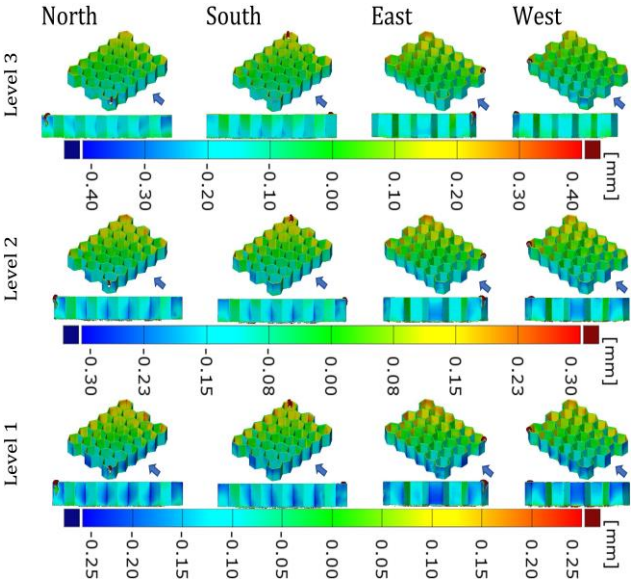

Fig 8. Scan results after splitting the honeycomb structure into three pieces.

In Fig 9., scan results of three pieces anti-tetrachiral lattice structure are shown. According to the results, no warpage syndrome can be seen at all levels. There are high deviations in the nodes and ligaments connection lines which can be explained as the scan error due to the lack of optic measurements in the narrow parts. Similar deviation patterns are seen at all levels.

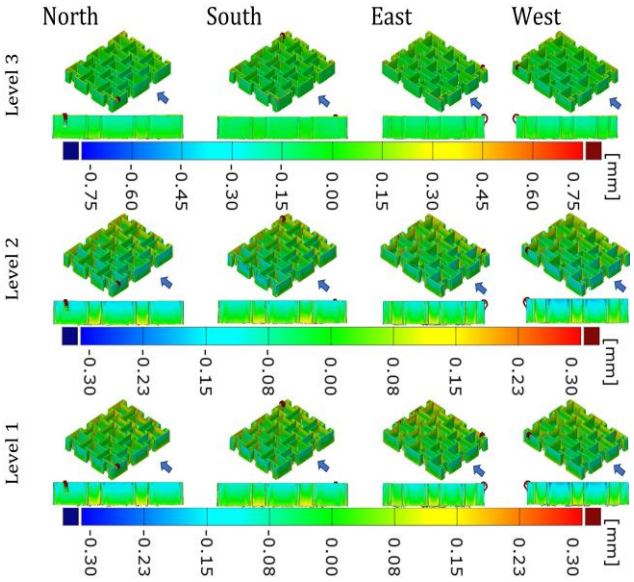

Fig 9. Scan results after splitting the anti-tetrachiral structure into three pieces

4. Conclusions

Three different thin-walled lattice structures were produced with DMLM from In718. Lattice structures were removed from the build plate and split into three equal structures with WEDM. Their geometrical deviations and distortion were measured with the bluelight scan device and numerical analysis was conducted. Numerical results showed acceptable results in the E and N directions, in which the re-coater effect is less. For better numerical results, fine meshes and calibration are necessary. In the split lattice structures, honeycomb showed better results due to its unique topology. Re-entrant lattice structure were experienced higher deviations owing to its sharp corners.

Acknowledgments

This study is supported by Technological and Scientific Council of Turkey (TUBITAK) under Technology and Innovation Support Program (Grant Number: 5158001).

Author's statement

Conflict of interest: Authors state no conflict of interest. Informed consent: Informed consent has been obtained from all individuals included in this study. Ethical approval: The research related to human use complies with all the relevant national regulations, institutional policies and was performed in accordance with the tenets of the Helsinki Declaration, and has been approved by the authors' institutional review board or equivalent committee.

References

1. Lakes, R., Advances in negative Poisson's ratio materials. Advenced Materials, 1993.5(4):p.293–296.
2. Prawoto, Y., Seeing auxetic materials from the mechanics point of view: a structural review on the negative Poisson's ratio. Computational Material Science. 2012;58:p.140–153.
3. Günaydin, K., et al., Experimental investigation of auxetic structures subjected to quasi static axial load. 2017 8th International Conference on Recent Advances in Space Technologies (RAST), 2017, p. 7–10.
4. Gunaydin, K., et al., Chiral-Lattice-Filled Composite Tubes under Uniaxial and Lateral Quasi-Static Load: Experimental Studies. Applied Sciences,. 2021.11(9).
5. Günaydın, K., et al., In-plane compression behavior of anti-tetrachiral and re-entrant lattices. Smart Material Structures, 2019.28(11):115028.
6. Günaydın, K., and H.S. Türkmen, In-Plane Quasi-Static Crushing Finite Element Analysis of Auxetic Lattices. 2019 9th International Conference on Recent Advances in Space Technologies (RAST). IEEE, 2019. p. 645–648.
7. Li, D., J. Ma, L. Dong, and R. S. Lakes Three-Dimensional Stiff Cellular Structures With Negative Poisson's Ratio. Phys Status Solidi, 2017.254(12):1600785.
8. Karnessis, N., and G. Burriesci, Uniaxial and buckling mechanical response of auxetic cellular tubes. Smart Material Structures, 2013.22(8):84008.
9. Dallago, M., et al., Effect of the geometrical defectiveness on the mechanical properties of SLM biomedical Ti6Al4V lattices. Procedia Structural Integrity, 2018.13:161–167.
10. Bartolomeu, F., et al., Additive manufactured porous biomaterials targeting orthopedic implants: A suitable combination of mechanical, physical and topological properties. Material Science Engineering C, 2020;107:110342.
11. Ran, Q., et al., Osteogenesis of 3D printed porous Ti6Al4V implants with different pore sizes. J Mech Behav Biomed Mater, 2018.84:1–11.
12. Wang, D., et al., Characteristics of typical geometrical features shaped by selective laser melting. J Laser Applications, 2017.29(2):22007.
13. Calignano, F., Investigation of the accuracy and roughness in the laser powder bed fusion process. Virtual Phys Prototyp., 2018.13(2):97–104.
14. Ahmed, A., et al., Dimensional quality and distortion analysis of thin-walled alloy parts of AlSi10Mg manufactured by selective laser melting. J Manuf Mater Process, 2019.3(2):51.
15. Yan, C., et al., Advanced lightweight 316L stainless steel cellular lattice structures fabricated via selective laser melting. Material Design, 2014.55:533–41.
16. Maran, S., I. G. Masters, and G. J. Gibbons, Additive Manufacture of 3D Auxetic Structures by Laser Powder Bed Fusion—Design Influence on Manufacturing Accuracy and Mechanical Properties.,Applied Sciences.,2020.10(21):7738.
17. Kouraytem, N., et al.. Dynamic-loading behavior and anisotropic deformation of pre-and post-heat-treated IN718 fabricated by laser powder bed fusion. Addit Manuf, 2020;33:101083.